Primordial non-Gaussianity and the CMB (& LSS) in the Standard Model of the Universe (II)

Sabino Matarrese
Dipartimento di Fisica "*Galileo Galilei*",
Università degli Studi di Padova, ITALY
email: sabino.matarrese@pd.infn.it

Paris Cosmology Colloquium 2009

Precision Cosmology: from “what” to “why”

- “Now that key cosmological parameters have been determined to within a few percent, we anticipate a generation of experiments that move beyond adding precision to measurements of what the universe is made of, but instead help us learn **why the universe has the form we observe**. […] observational cosmology will probe the detailed dynamics of the universe in the earliest instants after the Big Bang, and start to yield clues about the physical laws that governed that epoch. Future experiments will plausibly reveal the dynamics responsible both for the large-scale homogeneity and flatness of the universe, and for the primordial seeds of small-scale inhomogeneities, including our own galaxy.” (Baumann et al. 2008, *CMBpol mission concept study*)

Inflation and Observational Cosmology: where do we stand?

Label	Definition	Physical Origin	Current Status
A_s	Scalar Amplitude	V, V'	$(2.445 \pm 0.096) \times 10^{-9}$
n_s	Scalar Index	V', V''	0.960 ± 0.013
α_s	Scalar Running	V', V'', V'''	only upper limits
A_t	Tensor Amplitude	V (Energy Scale)	only upper limits
n_t	Tensor Index	V'	only upper limits
r	Tensor-to-Scalar Ratio	V'	only upper limits
Ω_k	Curvature	Initial Conditions	only upper limits
$f_{\rm NL}$	Non-Gaussianity	Non-Slow-Roll, Multi-Field	only upper limits
S	Isocurvature	Multi-Field	only upper limits
$G\mu$	Topological Defects	End of Inflation	only upper limits

The determination of most of these parameters requires the combination of LSS and CMB data on both large and small scales.

CMB: a Window to the Physics of the Early Universe

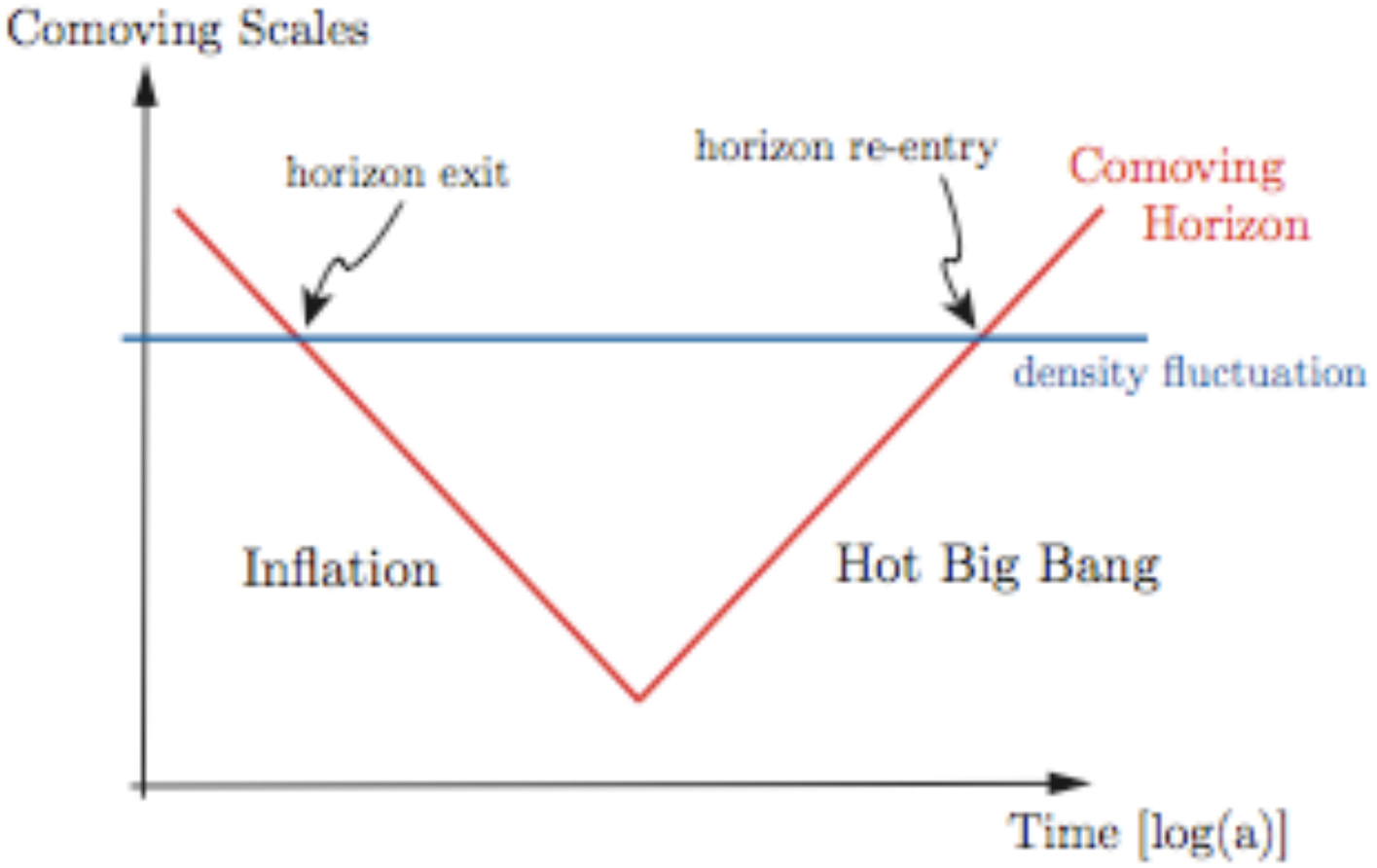

Testable predictions of inflation

- ✓ Cosmological aspects
  - Critical density Universe
  - Almost scale-invariant and nearly Gaussian, adiabatic density fluctuations
  - Almost scale-invariant stochastic background of relic gravitational waves

- ✓ Particle physics aspects
  - Nature of the inflaton
  - Inflation energy scale

Why (non-) Gaussian?

Gaussian ⟺ free (i.e. non-interacting) field

- collection of independent harmonic oscillators (no mode-mode coupling)
- the motivation for Gaussian initial conditions (the standard assumption) ranges from mere simplicity to the use of the Central Limit Theorem (e.g. Bardeen et al. 1986), to the property of inflation produced seeds (… see below)

large-scale phase coherence ⟺ non-linear gravitational dynamics

The view on Non-Gaussianity … circa 1990

Moscardini, Lucchin, Matarrese & Messina 1991

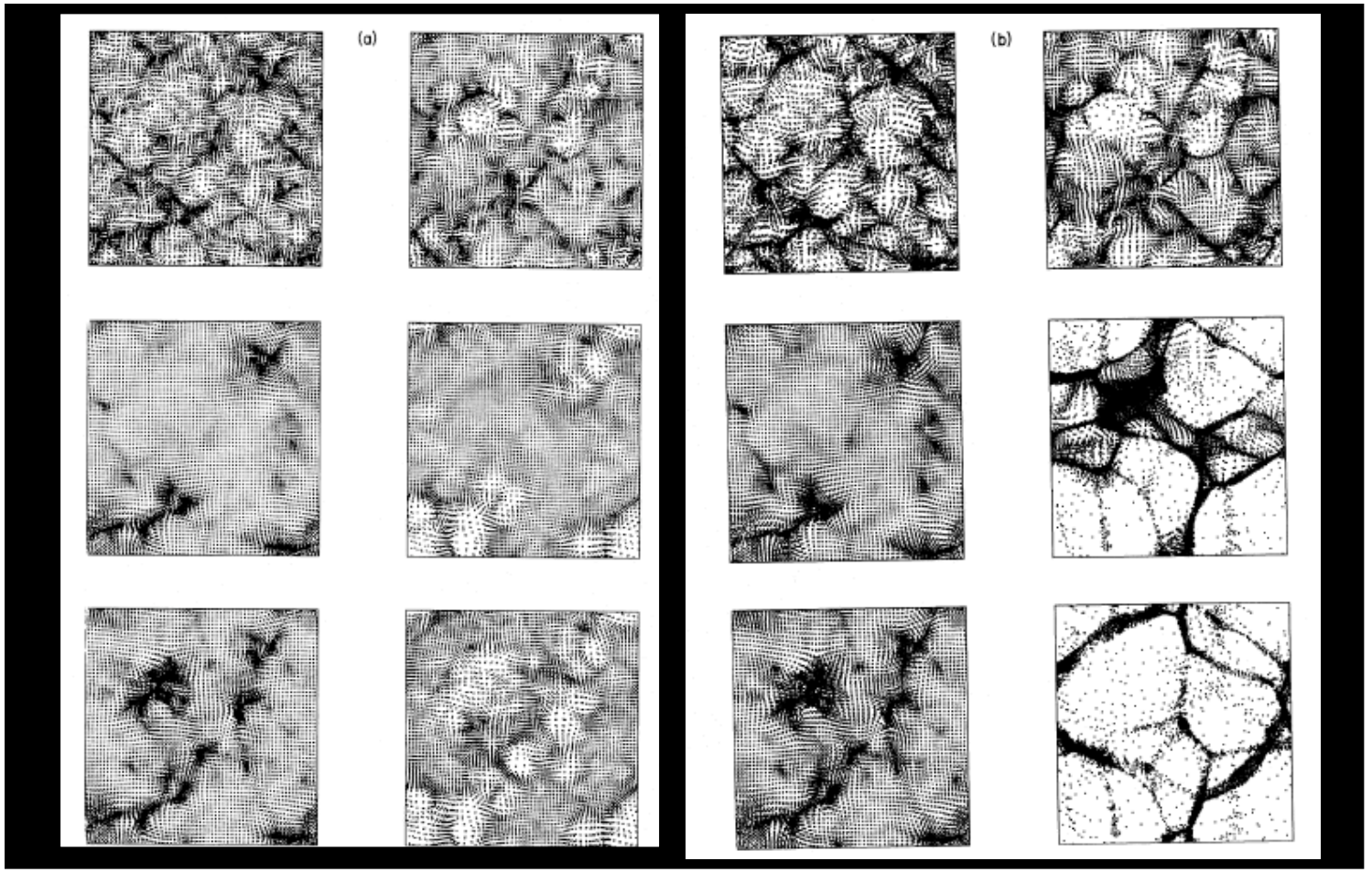

Non-Gaussianity

- Alternative structure formation models of the late eighties considered strongly non-Gaussian primordial fluctuations.
- The increased accuracy in CMB and LSS observations has excluded this extreme possibility.
- The present-day challenge is either detect or constrain mild or weak (~ 0.001%) deviations from primordial Gaussian initial conditions.
- Deviations of this type are not only possible but are generically predicted in the standard perturbation generating mechanism provided by inflation.

Simple-minded NG model

- ✓ Many primordial (inflationary) models of non-Gaussianity can be represented in configuration space by the simple formula (Salopek & Bond 1990; Gangui et al. 1994; Verde et al. 1999; Komatsu & Spergel 2001)

$$\Phi = \phi_L + f_{NL} * (\phi_L^2 - \langle \phi_L^2 \rangle) + g_{NL} * \phi_L^3 + \ldots$$

where Φ is the large-scale gravitational potential, ϕ_L its linear Gaussian contribution and f_{NL} is the dimensionless *non-linearity parameter* (or more generally *non-linearity function*). The percent of non-Gaussianity in CMB data implied by this model is

$$\text{NG \%} \sim 10^{-5} \; |f_{NL}|$$

$$\sim 10^{-10} \; |g_{NL}|$$

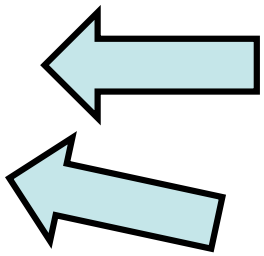

$< 10^{-4}$ from *WMAP*

$< 10^{-4}$ from *LSS*

NG as a Test on the Physics of the Early Universe

- The bispectrum (trispectrum, …) amplitude and shape measures deviations from standard inflation, perturbation generating processes after inflation, initial state before inflation, …. Going to small scales and exploiting E-mode polarization allows to reach very high sensitivity (small f_{NL}). Inflation models which would yield the same predictions for scalar spectral index and tensor-to-scalar ratio might be distuinguishable in terms of NG features. Can we aim at "reconstructing" the inflationary action, starting from measurements of a few observables (like n_S, r, n_T, f_{NL}, g_{NL}, etc. …), just like in the nineties we were aiming at a reconstruction of the inflationary potential?

- The statistics of E and B modes, sensitive to CMB lensed by LSS, hence allowing to improve limits on primordial (GW induced) B modes. Non-Gaussian GW background (from pre-heating after inflation, curvaton mechanism, phase-transitions, secondary GW background).

Inflation models and f_{NL}

Updated table from N. B., E. Komatsu, S. Matarrese and A. Riotto., Phys. Rept. 2004

model	$f_{NL}(k_1,k_2)$	comments
Standard inflation	$O(\varepsilon,\eta)$	
curvaton	$5/4r - 5r/6 - 5/3$	$r \sim (\rho_\sigma/\rho)_{decay}$
modulated reheating	$-5/4 - I$	$I = -5/2 + 5\Gamma/(12\,\alpha\Gamma_1)$ $I = 0$ (*minimal case*)
multi-field inflation	may be large ?	
Feature in the inflaton potential	$\lvert f_{NL} \rvert > 1$	
"unconventional" inflation set-ups		
DBI	$-0.32 / c_s^2$	*equilateral configuration*
Generalized single-field inflation (e.g:k-and brane inflation)	$-(35/108)(1/c_s^2-1)$ $+(5/81)(1/c_s^2-1-2\lambda/\Sigma)$	High when the sound of speed c_s $\ll 1$ or $\lambda/\Sigma \gg 1$
ghost inflation	$-85\,\beta\,\alpha^{-3/5}$	*equilateral configuration*

model	$f_{NL}(k_1,k_2)$	comments
Excited initial states+derivative interactions	~(6.3 10^{-4} M_{Pl}/M) ~(1-100)	Flatten configuration M: cut-off scale
Preheating scenarios	e.g. (M_{Pl}/φ_0) $e^{Nq/2}$ ~50	N:n° of inflaton oscillations
Inhomogeneous preheating And inhom. hybrid inflation	e.g. (5/6) λ_φ (M_{Pl}/m_χ)	λ_φ: inflaton coupling to the waterfall field χ
Warm inflation	typically 10^{-1}	
Warm Inflation (II)	$-15L(r) < f_{NL} < L(r)$	$L(r) \approx \ln(1+r/14)$; $r=\Gamma/3H >>1$
Ekpyrotic models	$-50 < f_{NL} < 200$	depends on the sharpness of conversion from isocurvature to curvature perturbations
Generalized slow-roll inflation (higher-order kinetic terms)	$f_{NL} >> +1$	equilateral configuration
Multi-DBI inflation	$f_{NL} \sim c_s^{-2}$ $1/(1+T^2_{RS})$	both local and equil. shapes

Inflation Models and g_{NL}

model	$g_{NL}(\mathbf{k}_1,\mathbf{k}_2)$	comments
Slow-roll inflation (including multiple fields)	$O(\varepsilon,\eta)$	ε,η : slow-roll parameters
Curvaton scenario	$(9/4\ r^2)\ (g^2\ g'''/g'^3+3g\ g''/g'^2)$ + - $(2/r)\ (1+\ 3g\ g''/g'^2)$	g'': deviation from a quadratic potential
Inhomogeneous reheating	$(5/3)\ f_{NL}^2+\ (25/24)\ (Q'''(x)/\ Q'^3(x))$	$X=\Gamma/H$ at the end of inflation
DBI inflation	$\sim 0.1\ c_s^{-4}$	C_s^2 : sound speed
Ekpyrotric models	$\lvert g_{NL}\rvert < 10^4$	depends on the parameter choice

NG (and anisotropy) from non-Abelian vector fields

- Bartolo, Dimastrogiovanni, Matarrese & Riotto, 2009

  – *Non-Gaussianity.* Primordial vector fields might generate a larger non-Gaussianity than the one observed in standard inflation.

  – *Anisotropy.* Violation of primordial rotational invariance from vector fields introduces some degree of anisotropy in the correlation functions.

  We generalize the Abelian case (Dimopoulos et al, arXiv:0809.1055), considering an $SU(2)$ gauge multiplet non-minimally coupled to gravity during inflation

$$S = \int d^4x\sqrt{-g}\Big[\frac{m_p^2 R}{2} - \frac{1}{4}g^{\mu\alpha}g^{\nu\beta}F^a_{\mu\nu}F^a_{\alpha\beta} - \frac{1}{2}\left(m^2+\xi R\right)g^{\mu\nu}B^a_\mu B^a_\nu + L_\phi\Big],$$

- Possible realizations: vector curvaton / vector inflation

- NG can be large and anisotropic

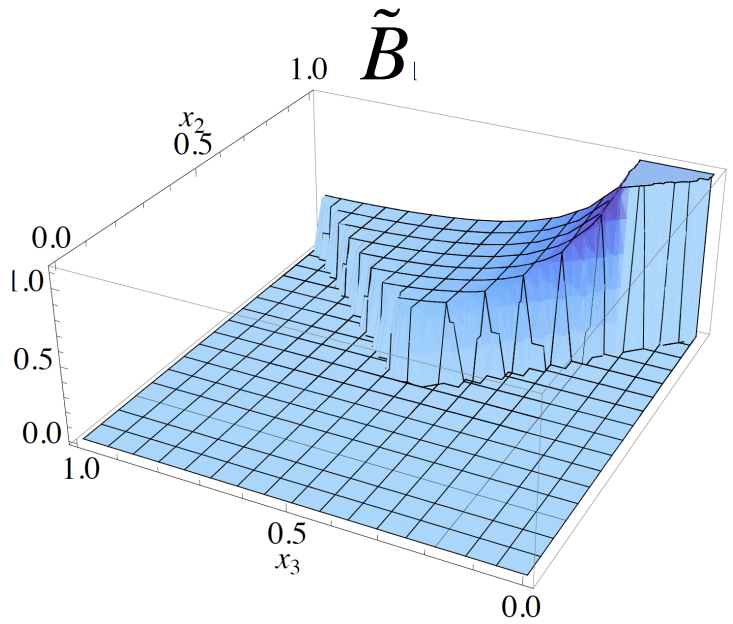

$$B(\vec{\mathbf{k}}_1,\vec{\mathbf{k}}_2,\vec{\mathbf{k}}_1) \sim \mathbf{I}(\vec{n}_i \bullet \vec{k}_i)\, \tilde{B}(\mathbf{k}_1,\mathbf{k}_2,\mathbf{k}_3)$$

→ Isotropic contribution to the bispectrum

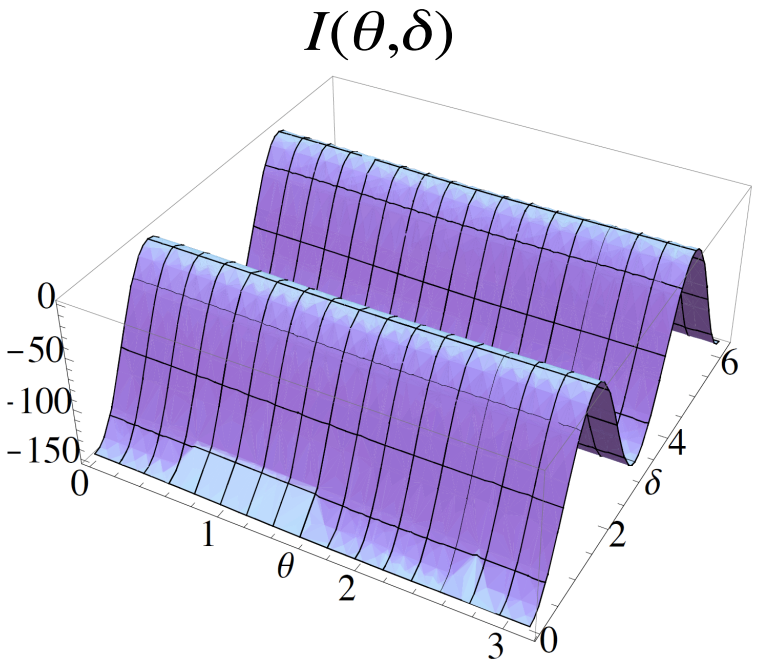

→ Modulation dependent on the preferred directions

Non-Gaussianity in the initial conditions

NG CMB simulated maps

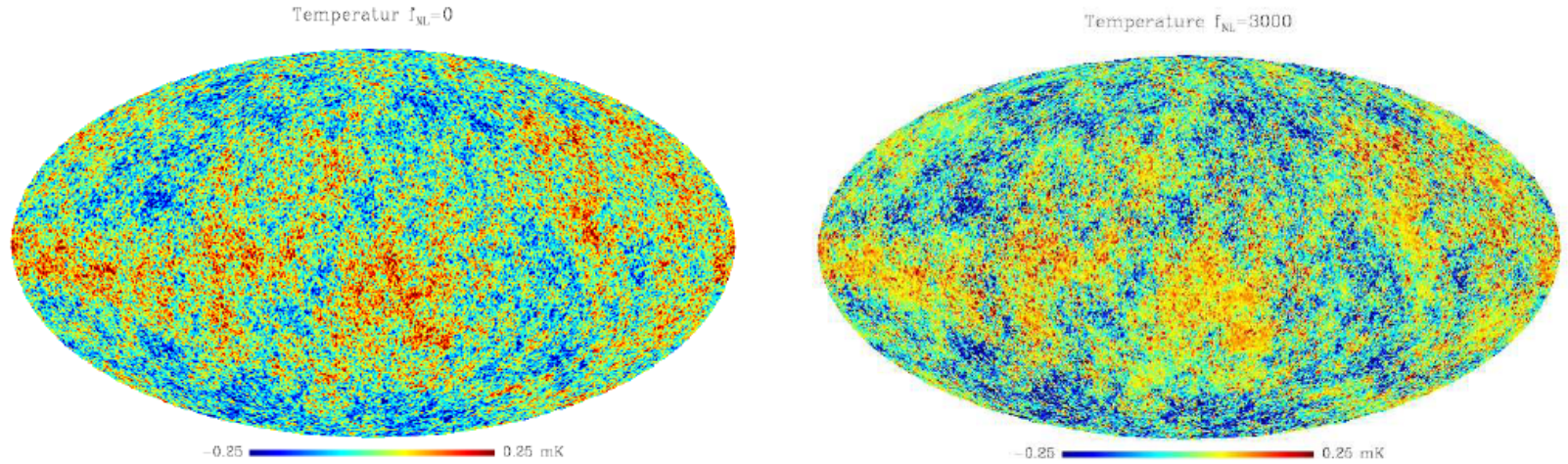

Liguori, Yadav, Hansen, Komatsu, Matarrese & Wandelt 2007

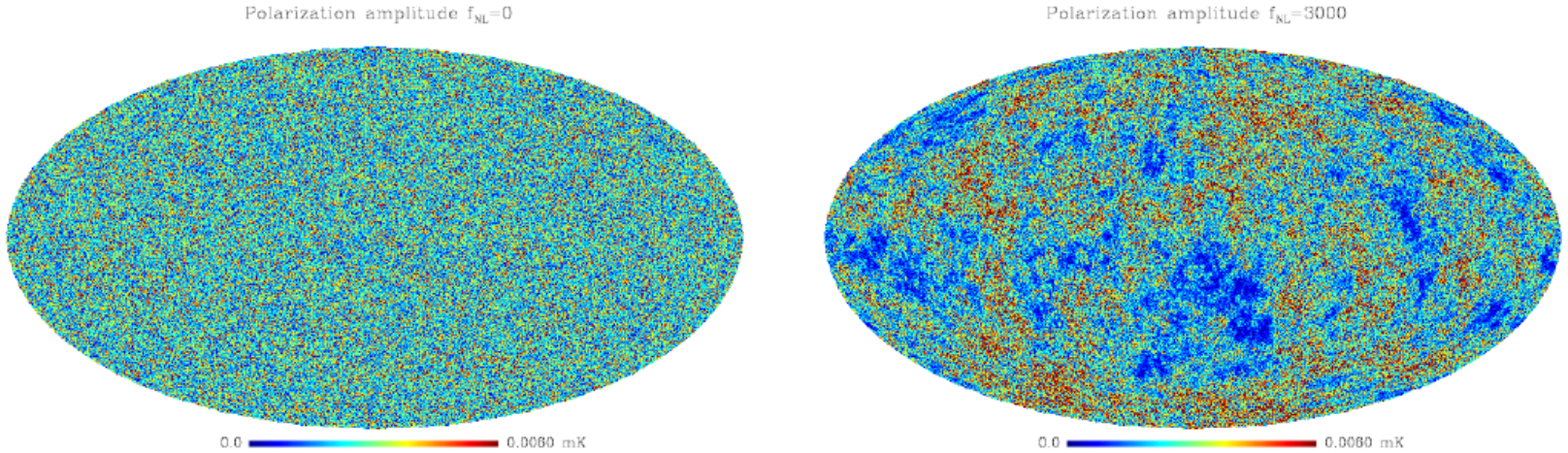

FIG. 8: Left column: temperature and polarization intensity Gaussian CMB simulations obtained from our algorithm. Polarization intensity is defined as $I \equiv \sqrt{Q^2 + U^2}$ where Q and U are the Stokes parameters. Right column: temperature and polarization non-Gaussian maps with the same Gaussian seed as in the left column and $f_{\rm NL} = 3000$. The reason for the choice of such a large $f_{\rm NL}$ is that we wanted to make non-Gaussian effects visible by eye in the figures. The cosmological model adopted for this plots is characterized by: $\Omega_b = 0.042$, $\Omega_{cdm} = 0.239$, $\Omega_L = 0.719$, $h = 0.73$, $n = 1$, $\tau = 0.09$. Temperatures are in mK.

Summary of NG from inflation

Bartolo, Matarrese & Riotto 2005; Boubeker, Creminelli, D'Amico, Noreña & Vernizzi 2009

$$\delta T/T = -(\Phi/3)$$

$$\Phi = \Phi_{\rm L} + f_{\rm NL} \star (\Phi_{\rm L})^2 + g_{\rm NL} \star (\Phi_{\rm L})^3,$$

leading contribution to bispectrum:

- Quadratic non-linearity on large-scales (up to ISW and 2-nd order tensor modes). Standard slow-roll inflation yields $a_{NL} \sim b_{NL} \sim 1$

Include SW + ISW up to 3-rd order

$$f_{\rm NL} = -\left[\tfrac{5}{3}(1-a_{\rm NL}) + \tfrac{1}{6}\right] + \left[3(\mathbf{k}_1\cdot\mathbf{k}_3)(\mathbf{k}_2\cdot\mathbf{k}_3)/k^4 - (\mathbf{k}_1\cdot\mathbf{k}_2)/k^2\right] \quad \text{- cos(2}\vartheta\text{)}$$

additional contribution to trispectrum (together with f_{NL}^2 terms):

- Cubic non-linearity on large-scales (up to ISW and 2-nd order tensor modes)

$$g_{\rm NL}(\mathbf{k}_1,\mathbf{k}_2,\mathbf{k}_3) = \tfrac{25}{9}(b_{\rm NL}-1) + \tfrac{25}{9}(a_{\rm NL}-1)\mathcal{A}(\mathbf{k}_1,\mathbf{k}_2,\mathbf{k}_3) + \tfrac{25}{9}\mathcal{C}(\mathbf{k}_1,\mathbf{k}_2,\mathbf{k}_3) - \tfrac{5}{9}(a_{\rm NL}-1)$$
$$+ \frac{1}{54} - \frac{1}{3}\left[\frac{(\mathbf{k}_1\cdot(\mathbf{k}_1+\mathbf{k}_2))\,(\mathbf{k}_2\cdot(\mathbf{k}_1+\mathbf{k}_2))}{|\mathbf{k}_1+\mathbf{k}_2|^4} - \frac{1}{3}\frac{\mathbf{k}_1\cdot\mathbf{k}_2}{|\mathbf{k}_1+\mathbf{k}_2|^2} + \text{cycl.}\right],$$

The shape of Non-Gaussianities

Different models for the generation of NG may lead to a different shape dependence of the bispectrum, which is very important for constraining NG

squeezed configurations dominant

equilateral configurations approximately dominant

Babich et al. 2005; Creminelli et al. 2005; LoVerde et al. 2007

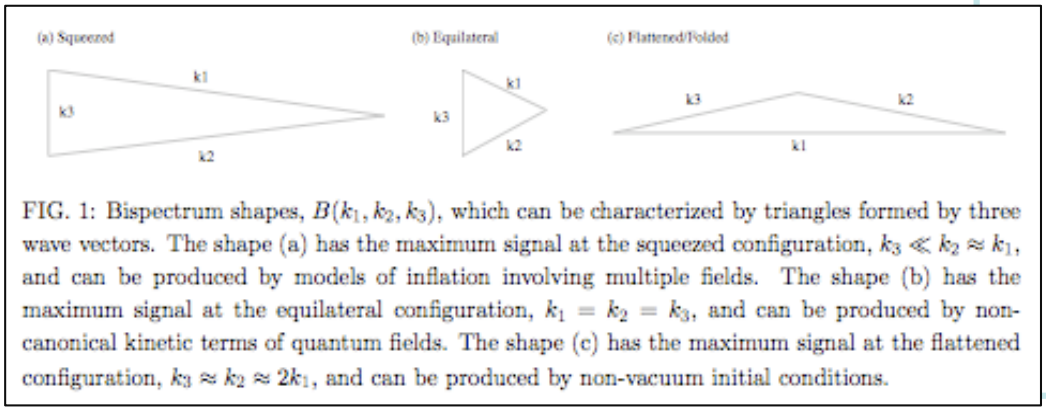

FIG. 1: Bispectrum shapes, $B(k_1, k_2, k_3)$, which can be characterized by triangles formed by three wave vectors. The shape (a) has the maximum signal at the squeezed configuration, $k_3 \ll k_2 \approx k_1$, and can be produced by models of inflation involving multiple fields. The shape (b) has the maximum signal at the equilateral configuration, $k_1 = k_2 = k_3$, and can be produced by non-canonical kinetic terms of quantum fields. The shape (c) has the maximum signal at the flattened configuration, $k_3 \approx k_2 \approx 2k_1$, and can be produced by non-vacuum initial conditions.

local

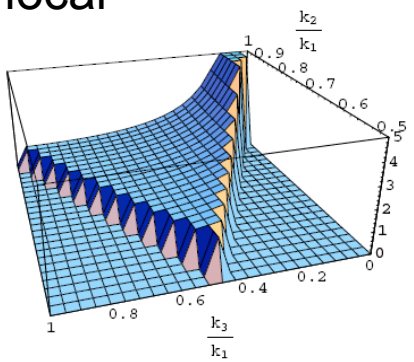

(a)

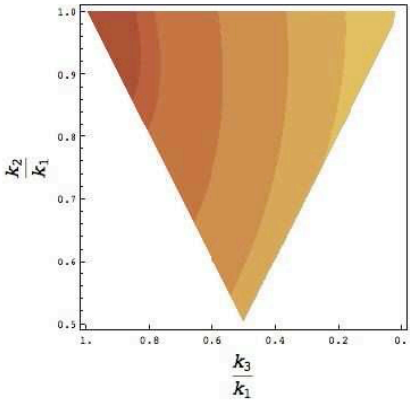

(b)

DBI

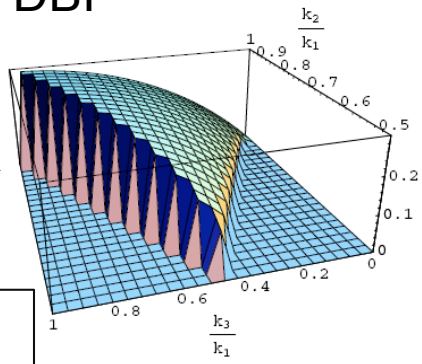

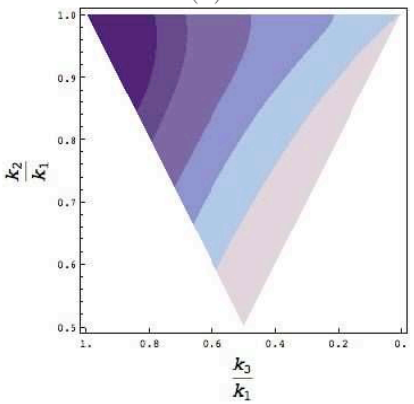

LoVerde et al. 2007

Figure 2: (a) The shape of the primordial bispectrum for the local model, $\mathcal{A}_{local}(1, k_2, k_3)/(k_2 k_3)/f_{NL}$. The domain of the plot is restricted to $\mathbf{k}_1 + \mathbf{k}_2 + \mathbf{k}_3 = 0$. (b) Contour plot of the fractional difference between the local form of non-Gaussianity and the DBI shape. Shaded regions show contours of (beginning from the upper left-hand corner) $(\mathcal{A}_{local} - \mathcal{A}_c)/\mathcal{A}_c$ =0, 0.05, 0.1, 0.5, 1, 2, 10. (c) The dominant shape in the primordial bispectrum for the DBI model, plotted is $\mathcal{A}_c(1, k_2, k_3)/(k_2 k_3)/f^c_{NL}$.(d) Contour plot of the fractional difference between the equilateral form of non-Gaussianity and the DBI shape. Shaded regions show contours of (beginning from the upper left-hand corner) $(\mathcal{A}_{equil} - \mathcal{A}_c)/\mathcal{A}_c = 0, 0.01, 0.02, 0.05, 0.1, 0.25$.

WMAP 5-yr limits on local models

✓ From an analysis of the bispectrum of CMB temperature anisotropies

$$-9 < f_{\rm NL}^{\rm loc} < 111 \ (95\%)$$

Komatsu et al. 2008

- from the template-cleaned V+W channel;
- accounting for a bias from unresolved point sources
- for

TABLE 5

CLEAN-MAP ESTIMATES AND THE CORRESPONDING 68% INTERVALS OF THE LOCAL FORM OF PRIMORDIAL NON-GAUSSIANITY, $f_{NL}^{\rm local}$, THE POINT SOURCE BISPECTRUM AMPLITUDE, b_{src} (IN UNITS OF 10^{-5} $\mu{\rm K}^3$ ${\rm sr}^2$), AND MONTE-CARLO ESTIMATES OF BIAS DUE TO POINT SOURCES, $\Delta f_{NL}^{\rm local}$

Band	Mask	$l_{\rm max}$	$f_{NL}^{\rm local}$	$\Delta f_{NL}^{\rm local}$	b_{src}
V+W	*KQ85*	400	50 ± 29	1 ± 2	0.26 ± 1.5
V+W	*KQ85*	500	61 ± 26	2.5 ± 1.5	0.05 ± 0.50
V+W	*KQ85*	600	68 ± 31	3 ± 2	0.53 ± 0.28
V+W	*KQ85*	700	67 ± 31	3.5 ± 2	0.34 ± 0.20
V+W	*Kp0*	500	61 ± 26	2.5 ± 1.5	
V+W	*KQ75p1*[a]	500	53 ± 28	4 ± 2	
V+W	*KQ75*	400	47 ± 32	3 ± 2	-0.50 ± 1.7
V+W	*KQ75*	500	55 ± 30	4 ± 2	0.15 ± 0.51
V+W	*KQ75*	600	61 ± 36	4 ± 2	0.53 ± 0.30
V+W	*KQ75*	700	58 ± 36	5 ± 2	0.38 ± 0.21

[a]This mask replaces the point-source mask in *KQ75* with the one that does not mask the sources identified in the *WMAP* K-band data

✓ See also Senatore et al. (2009)

$$-4 < f_{\rm NL}^{\rm loc} < 80 \ (95\%)$$

✓ and claimed evidence from Yadav & Wandelt 08, WMAP3

$$27 < f_{NL} < 147 \ (95\%)$$

WMAP 5yr limits on equilateral models

From an analysis of the bispectrum of CMB temperature anisotropies

$$-151 < f_{NL}^{\mathbf{equil}} < 253 \ (95\%)$$

Komatsu et al. 2008

for $l_{\max} = 700$

See also Senatore et al. (2009)

$$-125 < f_{\mathrm{NL}}^{\mathrm{equil}} < 435 \ (95\%)$$

TABLE 7
CLEAN-MAP ESTIMATES AND THE CORRESPONDING 68% INTERVALS OF THE EQUILATERAL FORM OF PRIMORDIAL NON-GAUSSIANITY, f_{NL}^{equil}, AND MONTE-CARLO ESTIMATES OF BIAS DUE TO POINT SOURCES, $\Delta f_{NL}^{\mathrm{equil}}$

Band	Mask	$l_{\max}$	f_{NL}^{equil}	$\Delta f_{NL}^{\mathrm{equil}}$
V+W	*KQ75*	400	77 ± 146	9 ± 7
V+W	*KQ75*	500	78 ± 125	14 ± 6
V+W	*KQ75*	600	71 ± 108	27 ± 5
V+W	*KQ75*	700	73 ± 101	22 ± 4

Constraining Non-Gaussianity from Inflation with Planck vs. ideal experiment

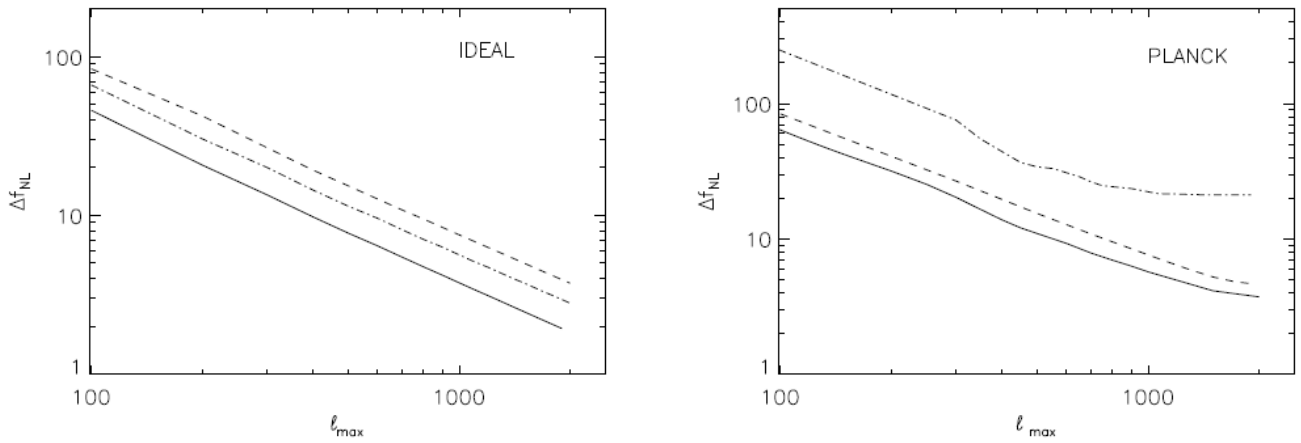

Fig. 2.— Fisher predictions for minimum detectable f_{NL} at the 1-σ level. Left panel: ideal experiment. Right panel: Planck satellite. Solid lines: temperature and polarization information combined. Dashed lines: temperature information only. Dot-dashed line: polarization information only.

Yadav, Komatsu and Wandelt 2007

Searching for NG in Planck data will require accurate handling of residual NG from systematics (foreground, point sources, NG induced by map making).

Fast estimator extended to incomplete sky coverage in Yadav, Komatsu, Wandelt, Liguori, Hansen & Matarrese 2007: see also Creminelli, Nicolis, Senatore & Tegmark 2006; covariance weighted KSW estimator used by Senatore, Smith & Zaldarriaga 2009

Fast estimation of localized f_{NL} values

Rudjord et al. 2009 (arXiv 0906.3232)

- Using the needlet f_{NL} estimator, one can divide the sky into several small pieces and obtain local estimates almost at the cost of one single full-sky f_{NL} estimation

- Using local estimates one can detect the influence of foregrounds and other systematic effects in certain parts of the sky

Local estimates (45 deg. disks) for WMAP V+W band

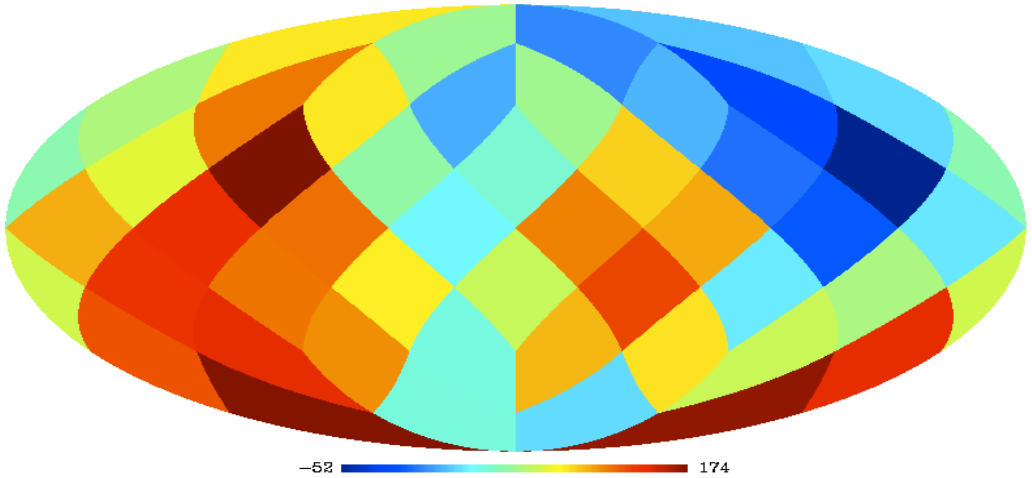

In WMAP data we found exceptionally high values of f_{NL} in local estimates close to galactic plane using Q-band, indicating foreground residuals with high significance.

Latest theoretical developments

Assessment of NG induced by secondary (second-order) anisotropies:

- Pitrou et al. 2008 vs. Bartolo & Riotto 2009 → *undetectable*
- Senatore, Tassev & Zaldarriaga 2009 vs. Khatri and Wandelt 2008, 2009 → *undetectable?*
- Nitta, Komatsu, Bartolo, Matarrese & Riotto 2009: no (previously unknown) 2nd order anisotropies (coming made of products of 1st x 1st order terms) can contaminate (local) NG at detectable level (good news!)
- Largest signal: cross-correlation of **lensing/ISW**: equivalent to local f_{NL}~10 (Mollerach & Matarrese 1997; Goldberg & Spergel 1999; Verde & Spergel 2002; Giovi et al. 2003; Smith & Zaldarriaga 2006; Serra & Cooray 2008; Hanson et al. 2009) **lensing/RS** (Mangilli & Verde 2009). We can subtract it (or use *constrained* N-body simulations to map it.

Open issues

- How to get the “right” bispectrum shape? Can we do anything better than chosing *a priori* the NG shape and then constrain f_{NL}?
- What is the optimal estimator of f_{NL} if, e.g., cubic NG (g_{NL}) is also there?
- Will we ever be able to improve our limits on f_{NL} with CMB data only?

Non-Gaussianity from initial conditions

+

Non-Gaussianity from gravitational instability

NG effects in LSS

- Bartolo, Matarrese & Riotto (2005) computed the effects of NG in the dark matter density fluctuations in a matter-dominated universe. Only for high values of f_{NL} (~10) the standard parameterization is valid. For smaller primordial NG strength non-Newtonian gravitational terms shift f_{NL} by a term ~ - 2 which depends on shape. On small scales stagnation effects during radiation dominance have to be taken into account up to second order. (Bartolo, Matarrese & Riotto 2007; Creminelli et al. 2008; Senatore et al. 2009).

- Sefusatti & Komatsu (2007) show that LSS becomes competitive with CMB at $z > 2$; Jeong & Komatsu (2009) and Sefusatti (2009) compute one-loop bispectrum of biassed objects.

NG and LSS

NG in LSS (to make contact with the CMB definition) can be defined through a potential Φ defined starting from the DM density fluctuation δ through Poisson's equation (use comoving gauge for density fluctuation, Bardeen 1980)

$$\delta = -\left(\frac{3}{2}\Omega_m H^2\right)^{-1} \nabla^2 \Phi$$

Many primordial (inflationary) models of non-Gaussianity can be represented in configuration space by the simple formula (Salopek & Bond 1990; Gangui et al. 1994; Verde et al. 1999; Komatsu & Spergel 2001)

$$\Phi = \phi_L + f_{NL}(\phi_L^2 - \langle \phi_L^2 \rangle) + g_{NL}\phi_L^3 + \ldots$$

Φ on sub-horizon scales reduces to minus the large-scale gravitational potential, ϕ_L its linear Gaussian contribution and f_{NL} is a dimensionless non-linearity parameter (or more generally non-linearity function). For $|f_{NL}| >> 1$ this definition is indentical to the CMB (up to a normalization factor ~ 1.3 coming from DE driven evolution of the linear gravitational potential).

Grossi et al. 2007

10 Mpc/h

Slices

$z = 0$

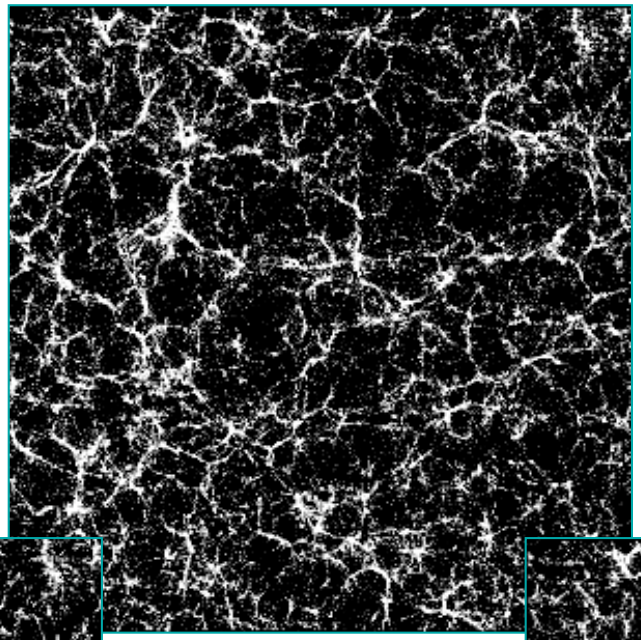

$f_{NL} = 0$

Gaussian model

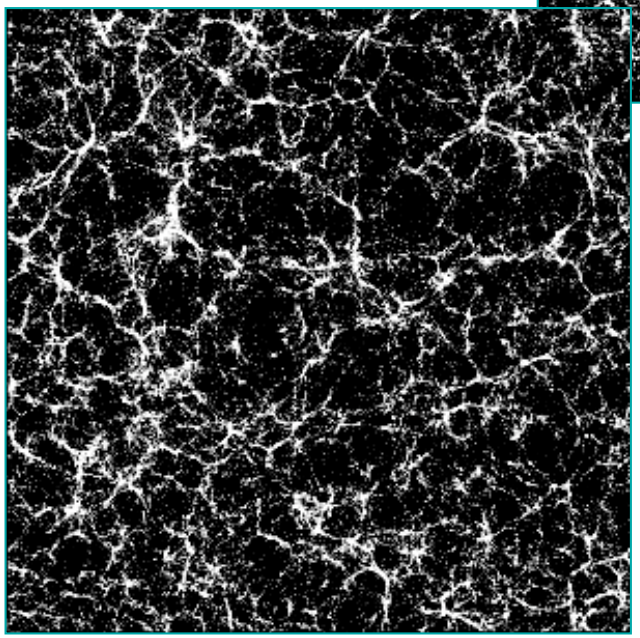

$f_{NL} = -1000$

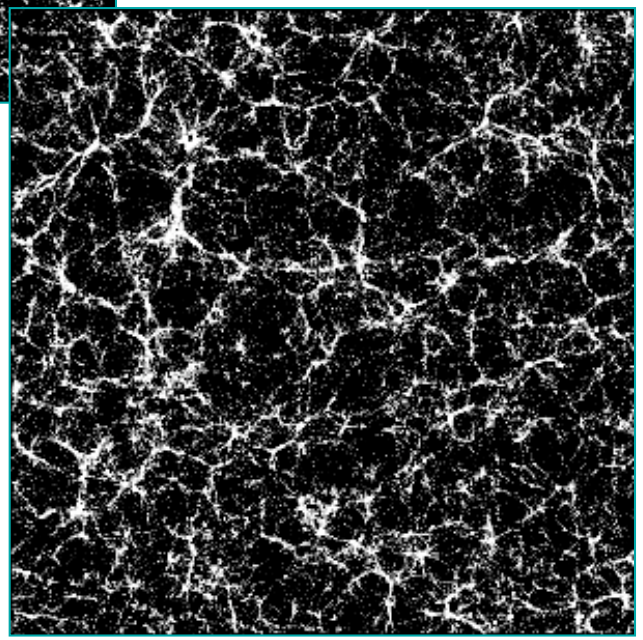

$f_{NL} = +1000$

N-body simultions with Non-Gaussian initial data

$$\Phi = \Phi_L + f_{NL}(\Phi_L^2 - \langle \Phi_L^2 \rangle)$$

$$\nabla^2(\Phi * T)g(z) = -4\pi G a^2 \delta\rho_{DM}$$

growth suppression factor

matter transfer function

Grossi et al. 2007, Hikage et al. 2007

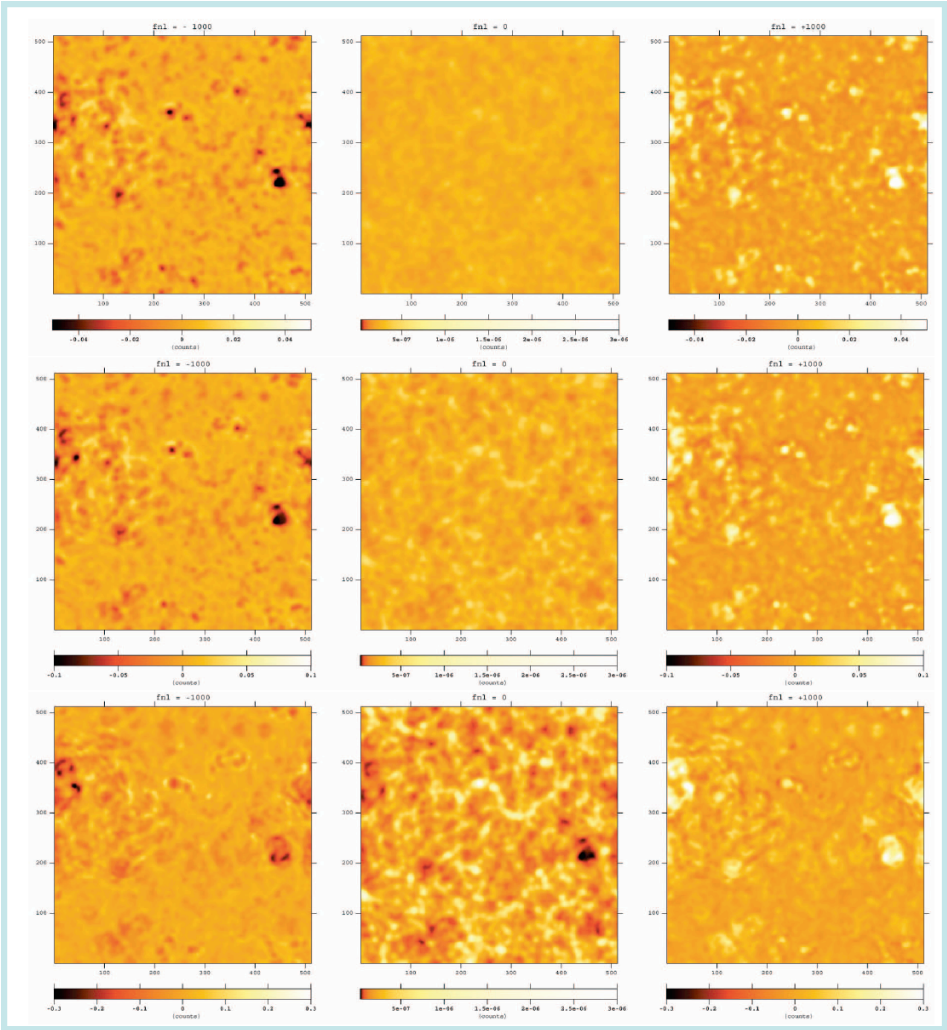

Figure 1. Slice maps of simulated mass density fields at $z = 5.15$ (*top*), $z = 2.13$ (*middle*) and $z = 0$ (*bottom*). The number of pixels at a side length is 512 ($500h^{-1}$Mpc) and that of the thickness is 32 ($31.25h^{-1}$Mpc). The panels in the middle row show the log of the projected density smoothed with a Gaussian filter of 10 pixels width, corresponding to $9.8h^{-1}$Mpc. The left and right panels are the relative residuals for the $f_{\rm NL}$=$\pm$1000 runs (equation [17]). Each panel has the corresponding color bar and the range considered are different from panel to panel.

Fitting NG with log-normal PDF

robust void statistics needed!

Grossi et al. 2008

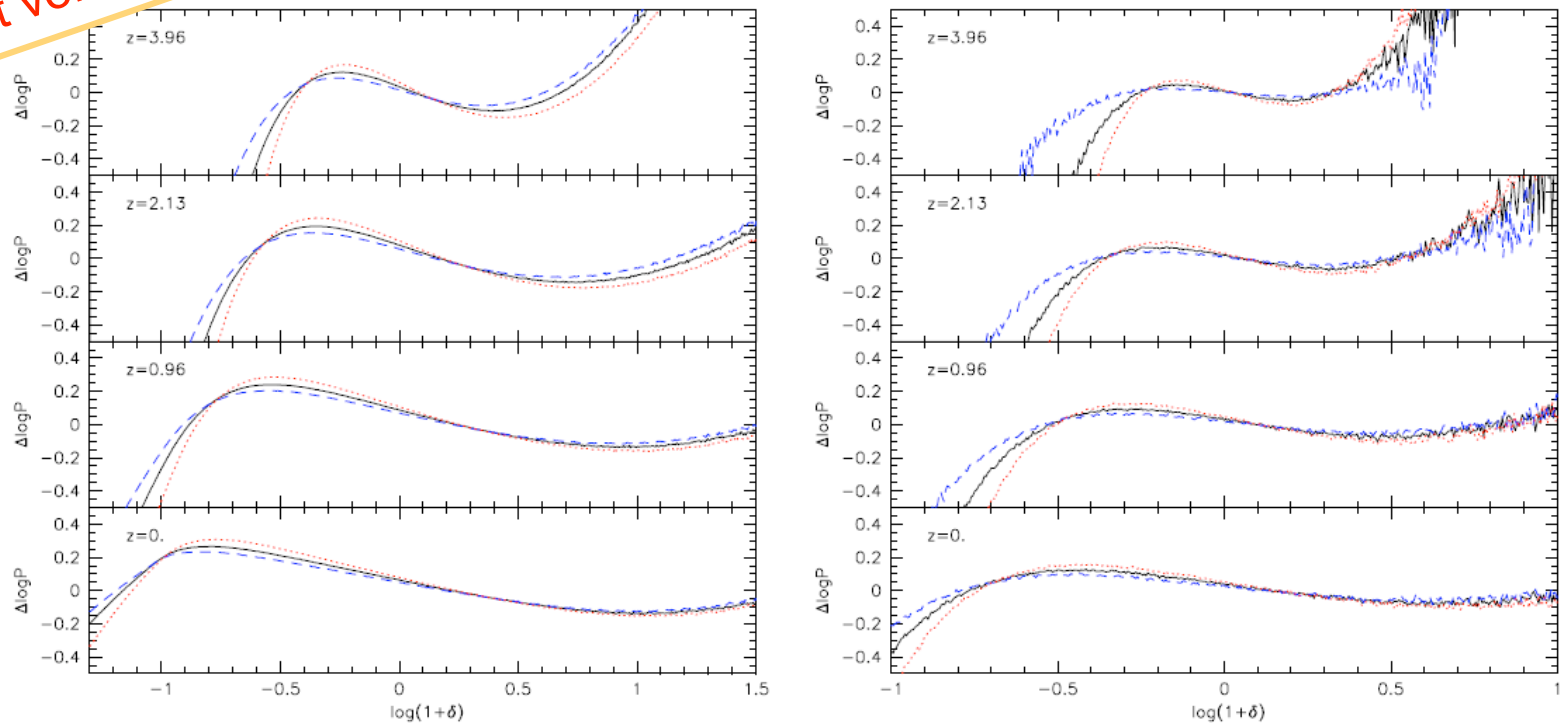

Figure 6. The logarithmic deviation of PDF from a lognormal distribution, $\Delta \log P$, is shown for the same models and redshifts presented in Fig. 5. Results for smoothing radii of $R_s \sim 0.98$ and $R_s \sim 3.91$ Mpc/h are displayed in left and right panels, respectively. Different lines refer to models with different primordial non-Gaussianity: $f_{\rm NL} = 0$ (solid line), $f_{\rm NL} = 1000$ (dotted line), $f_{\rm NL} = -1000$ (dashed line).

see also: Kamionkowski, Jimenez & Verde 2008

Searching for non-Gaussianity with rare events

- Besides using standard statistical estimators, like bispectrum, trispectrum, three and four-point function, skewness, etc. …, one can look at the tails of the distribution, i.e. at rare events.

- Rare events have the advantage that they often maximize deviations from what predicted by a Gaussian distribution, but have the obvious disadvantage of being rare! But remember that, according to Press-Schechter-like schemes, all collapsed DM halos correspond to (rare) peaks of the underlying density field.

- Matarrese, Verde & Jimenez (2000) and Verde, Jimenez, Kamionkowski & Matarrese showed that clusters at high redshift ($z>1$) can probe NG down to $f_{NL} \sim 10^2$ which is, however, not competitive with future CMB (Planck) constraints.

- Alternative approach by LoVerde et al. (2007). Determination of mass function using stochastic approach (first-crossing probability of a diffusive barrier) Maggiore & Riotto 2009. Ellispsoidal collapse used by Lam & Sheth 2009.

- Excellent agreement of analytical formulae with N-body simulations found by Grossi et al. 2009

DM halos in NG simulations

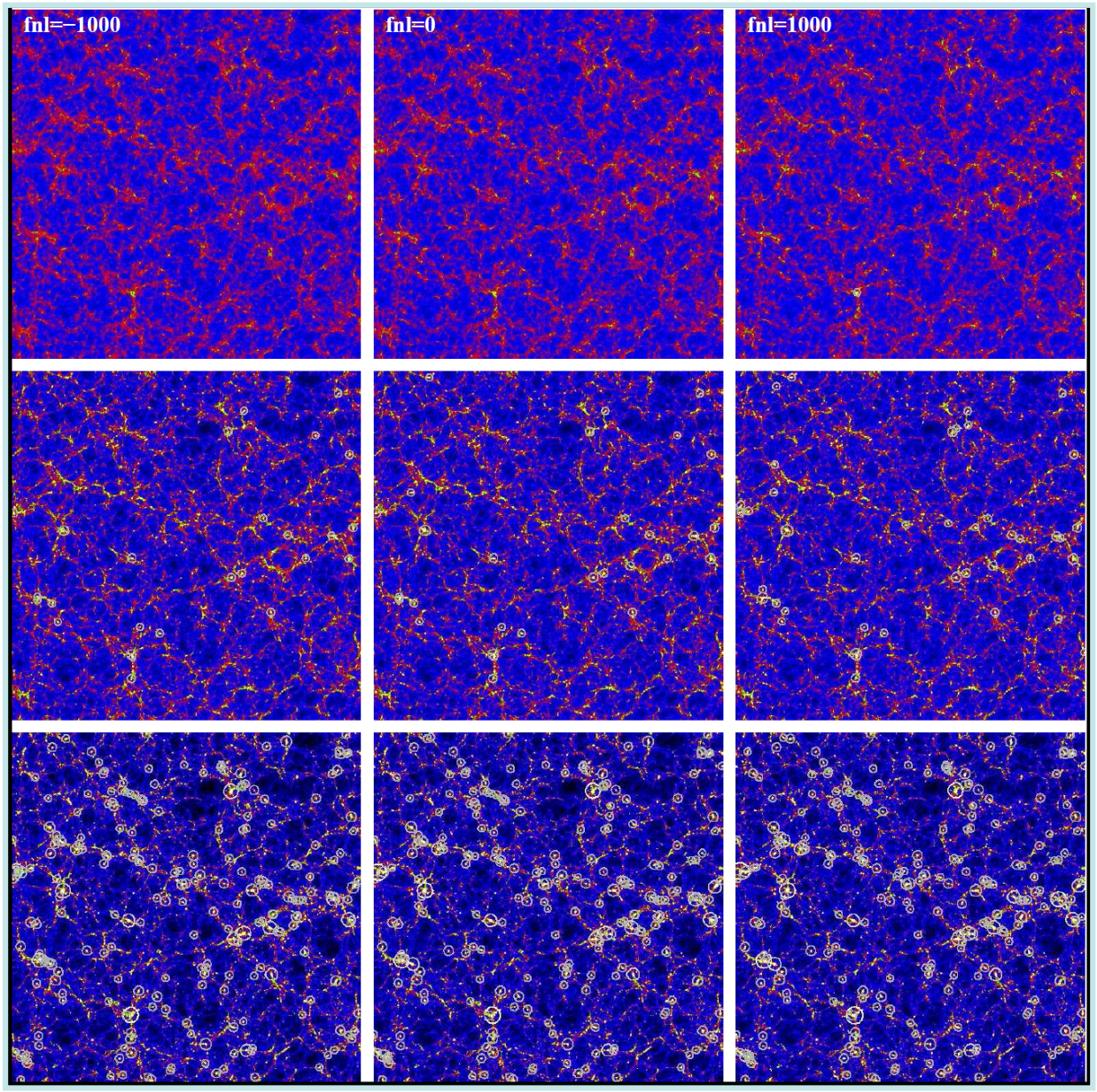

Grossi et al. 2008

DM halo mass function vs f_{NL}

Theoretical mass-function for quadratic NG field: Matarrese, Verde & Jimenez 2000, using a saddle-point technique; LoVerde et al. 2008, using Edgeworth expansion; Maggiore & Riotto 2009, using diffusing barrier; Lam & Sheth 2009 use Edgeworth exp. + ellipsoidal collapse barrier. Valageas 2009

Comparison with simulations in Desjacques et al. 2008; Pillepich et al. 2008; Grossi et al. 2009

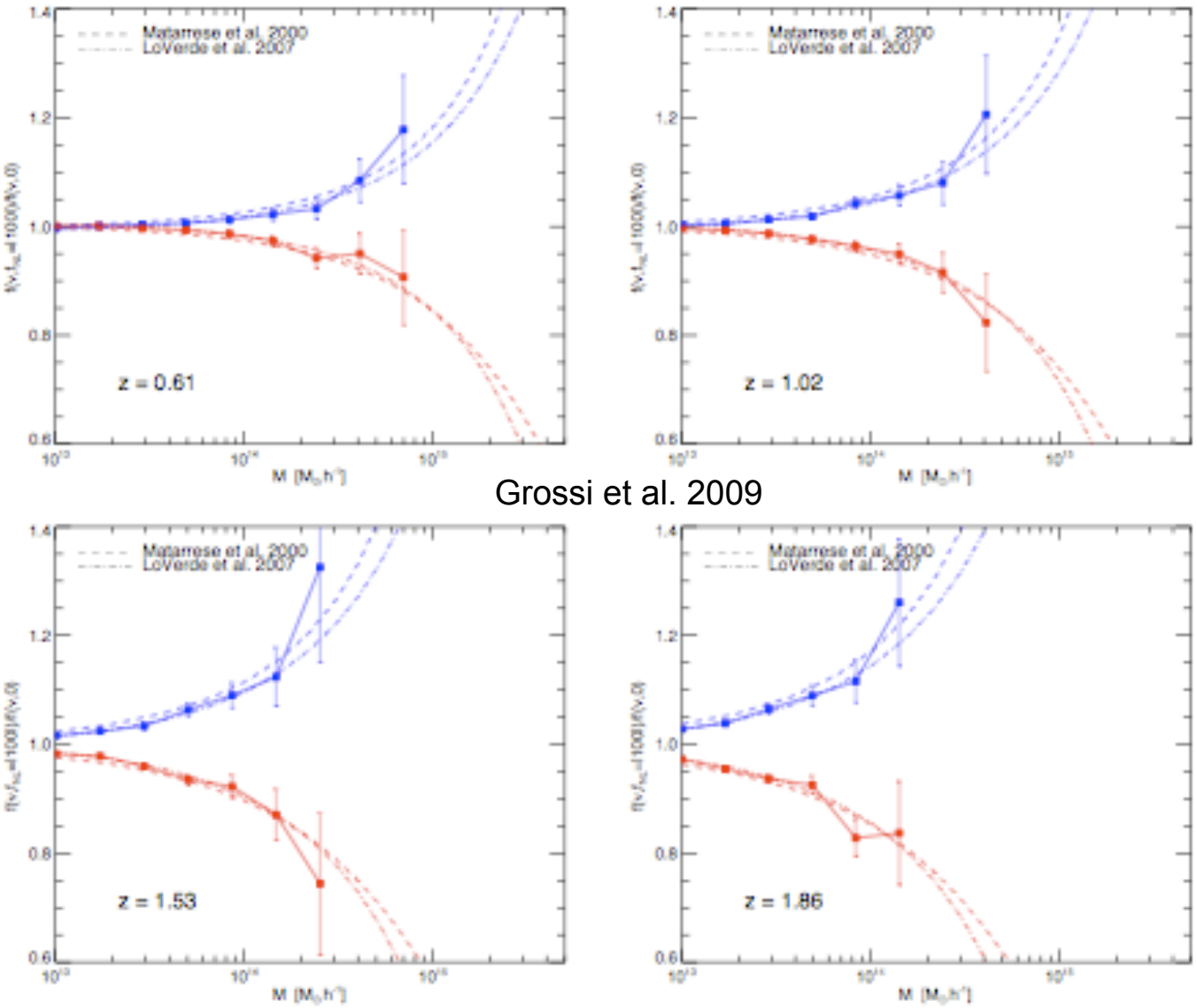

Grossi et al. 2009

Figure 6. Ratio of the non-Gaussian ($f_{NL} = \pm 100$) to Gaussian mass function for different redshift snapshots: top left $z = 0.61$; top right $z = 1.02$; bottom left $z = 1.53$; bottom right $z = 1.86$. The dashed line is the mass function of Matarrese, Verde & Jimenez (2001) and the dot-dashed lines are that of LoVerde et al. (2008), both including the q-correction.

DM halo clustering as a constraint on NG

$$\delta_{halo} = b\, \delta_{matter}$$

Dalal et al. (2007) have shown that halo bias is sensitive to primordial non-Gaussianity through a scale-dependent correction term

$$\Delta b(k)/b \;\alpha\; 2\, f_{NL} \delta_c / k^2$$

This opens interesting prospects for constraining or measuring NG in LSS but demands for an accurate evaluation of the effects of (general) NG on halo biasing.

Dalal, Dore', Huterer & Shirokov 2007

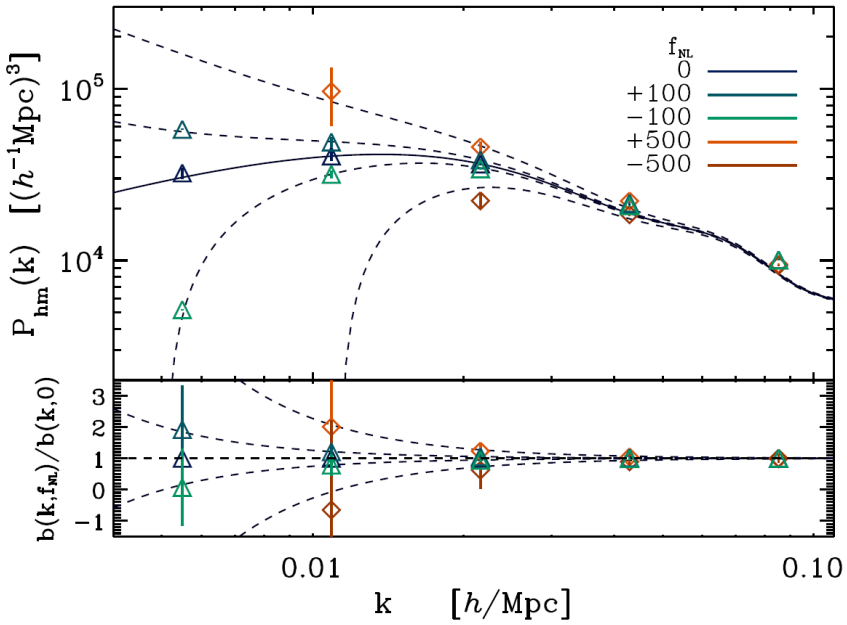

Clustering of peaks (DM halos) of NG density field

Start from results obtained in the 80's by

Grinstein & Wise 1986, ApJ, 310, 19

Matarrese, Lucchin & Bonometto 1986, ApJ, 310, L21

giving the general expression for the peak 2-point function as a function of N-point connected correlation functions of the background linear (i.e. Lagrangian) mass-density field

$$\xi_{h,M}(|\mathbf{x}_1 - \mathbf{x}_2|) = -1 + \exp\left\{ \sum_{N=2}^{\infty} \sum_{j=1}^{N-1} \frac{\nu^N \sigma_R^{-N}}{j!(N-1)!} \xi^{(N)} \begin{bmatrix} \mathbf{x}_1,\ldots,\mathbf{x}_1, & \mathbf{x}_2,\ldots\ldots,\mathbf{x}_2 \\ j\,times & (N-j)\,times \end{bmatrix} \right\}$$

(requires use of path-integral, cluster expansion, multinomial theorem and asymptotic expansion). The analysis of NG models was motivated by a paper by Vittorio, Juszkiewicz and Davis (1986) on bulk flows.

THE ASTROPHYSICAL JOURNAL, 310:L21–L26, 1986 November 1

A PATH-INTEGRAL APPROACH TO LARGE-SCALE MATTER DISTRIBUTION ORIGINATED BY NON-GAUSSIAN FLUCTUATIONS

SABINO MATARRESE
International School for Advanced Studies, Trieste, Italy
FRANCESCO LUCCHIN
Dipartimento di Fisica G. Galilei, Padova, Italy
AND
SILVIO A. BONOMETTO
International School for Advanced Studies, Trieste, Italy; Dipartimento di Fisica G. Galilei, Padova, Italy; and INFN, Sezione di Padova
Received 1986 July 7; accepted 1986 August 1

ABSTRACT

The possibility that, in the framework of a biased theory of galaxy clustering, the underlying matter distribution be non-Gaussian itself, because of the very mechanisms generating its present status, is explored. We show that a number of contradictory results, seemingly present in large-scale data, in principle can recover full coherence, once the requirement that the underlying matter distribution be Gaussian is dropped. For example, in the present framework the requirement that the two-point correlation functions vanish at the same scale (for different kinds of objects) is overcome. A general formula, showing the effects of a non-Gaussian background on the expression of three-point correlations in terms of two-point correlations, is given.

Subject heading: galaxies: clustering

THE ASTROPHYSICAL JOURNAL, 310:19–22, 1986 November 1

NON-GAUSSIAN FLUCTUATIONS AND THE CORRELATIONS OF GALAXIES OR RICH CLUSTERS OF GALAXIES[1]

BENJAMIN GRINSTEIN[2] AND MARK B. WISE[3]
California Institute of Technology
Received 1986 March 6; accepted 1986 April 18

ABSTRACT

Natural primordial mass density fluctuations are those for which the probability distribution, for mass density fluctuations averaged over the horizon volume, is independent of time. This criterion determines that the two-point correlation of mass density fluctuations has a Zeldovich power spectrum (i.e., a power spectrum proportional to k at small wavenumbers) but allows for many types of reduced (connected) higher correlations. Assuming galaxies or rich clusters of galaxies arise wherever suitably averaged natural mass density fluctuations are unusually large, we show that the two-point correlation of galaxies or rich clusters of galaxies can have significantly more power at small wavenumbers (e.g., a power spectrum proportional to $1/k$ at small wavenumbers) than the Zeldovich spectrum. This behavior is caused by the non-Gaussian part of the probability distribution for the primordial mass density fluctuations.

Subject headings: cosmology — galaxies: clustering

Peaks of NG random fields

- For a D-dimensional random field ε, filtered on scale R one defines a "peak operator"

$$n_{>\nu}(\mathbf{x},R) = \int_D d\omega (-1)^D \det\omega \;\; \Theta_H(\varepsilon_R(\mathbf{x}) - \nu\sigma_R)\delta^{(D)}(\partial_i\varepsilon_R(\mathbf{x}))\delta^{(D(D+1)/2)}(\partial_i\partial_j\varepsilon_R(\mathbf{x}) - \omega_{ij})$$

where one considers only peaks with heigth ilarger than ν times the rms fluctuation (on scale R). Here the domain D is over all negative definite symmetric matrices. For high threshold ν one expect one peak for every up-crossing region. In such a case one can compute the N-point function of $n_{>\nu}$ by standard QFT techniques (path-integral + cluster expansion) finding the N-point joint up-corssing probability (Matarrese, Lucchin & Bonometto 1986)

$$\Pi^{(N)}_{\nu,R} = (2\pi)^{-N/2}\int_\nu^\infty d\alpha_1 \cdots \int_\nu^\infty d\alpha_N \exp\left[\sum_{n=2}^{\infty}(-1)^n \sum_{[r_n]=1}^{N}\left(w^{(n)}_{R,[r_n]}/n!\right)\prod_{j=1}^{n}\left(\partial/\partial\alpha_{r_j}\right)\right] \times \exp\left[-(1/2)\sum_{r=1}^{N}\alpha_r^2\right]$$

with

$$a_0(z) = (1/2)\,\mathrm{erfc}(z)$$

$$a_m(z) = \pi^{-1/2}2^{-m/2}\,e^{-z^2}H_{m-1}(z) \qquad (m>0)$$

and

$$w^{(2)}_{R,[r_2]} = \xi^{(2)}_R(x_{r_1}, x_{r_2})/\sigma_R^2 \qquad (r_1 \neq r_2)$$

$$w^{(2)}_{R,[r_2]} = 0 \qquad (r_1 = r_2)$$

$$w^{(n)}_{R,[r_n]} = \xi^{(n)}_R(x_{r_1},\ldots,x_{r_n})/\sigma_R^n \qquad (n>2)$$

Halo bias in NG models

- Matarrese & Verde 2008 have applied this relation to the case of local NG of the gravitational potential, obtaining the power-spectrum of dark matter halos modeled as high "peaks" (up-crossing regions) of height $\nu=\delta_c/\sigma_R$ of the underlying mass density field (Kaiser's model). Here $\delta_c(z)$ is the critical overdensity for collapse (at redshift a) and σ_R is the *rms* mass fluctuation on scale R ($M \sim R^3$)

- Next, account for motion of peaks (going from Lagrangian to Eulerian space), which implies (Catelan et al. 1998)

$$1+\delta_h(\mathbf{x}_{Eulerian}) = (1+\delta_h(\mathbf{x}_{Lagrangian}))(1+\delta_R(\mathbf{x}_{Eulerian}))$$

  and (to linear order) $b=1+b_L$ (Mo & White 1996) to get the scale-dependent halo bias in the presence of NG initial conditions.

- Similar formulae apply to the correlation of CMB hot & cold spots (Heavens, Liguori, Matarrese, Tojeiro & Verde, in prep.)

- Alternative approach (based on 1-loop calculations by Taruya et al. (2008)

Halo bias in NG models

Matarrese & Verde 2008

$$b_{\rm h}^{f_{\rm NL}} = 1 + \frac{\Delta_c(z)}{\sigma_R^2 D^2(z)} \left[1 + 2 f_{\rm NL} \frac{\Delta_c(z)}{D(z)} \frac{\mathcal{F}_R(k)}{\mathcal{M}_R(k)} \right]$$

form factor:

$$\mathcal{F}_R(k) = \frac{1}{8\pi^2 \sigma_R^2} \int dk_1 k_1^2 \mathcal{M}_R(k_1) P_\phi(k_1) \times \int_{-1}^{1} d\mu \mathcal{M}_R\left(\sqrt{\alpha}\right) \left[\frac{P_\phi\left(\sqrt{\alpha}\right)}{P_\phi(k)} + 2 \right]$$

$$\alpha = k_1^2 + k^2 + 2 k_1 k \mu$$

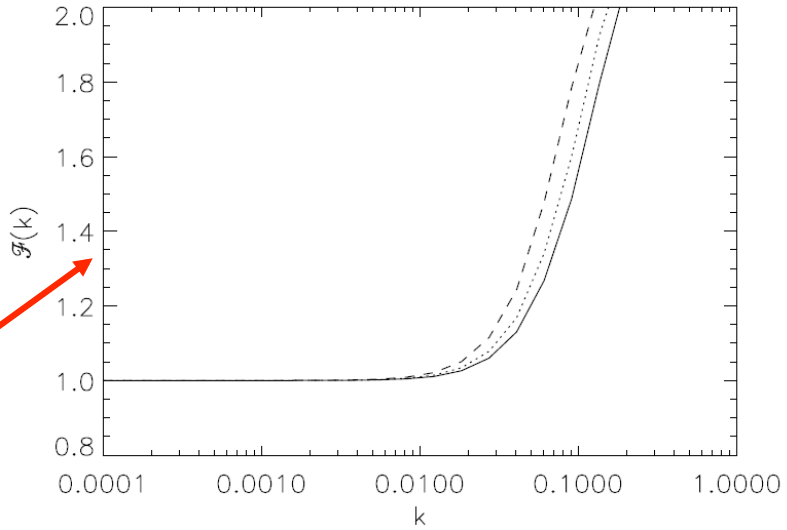

FIG. 1.— The function $\mathcal{F}_R(k)$ for three different masses: 1×10^{14} $M_\odot$ (solid), 2×10^{14} $M_\odot$ (dotted), 1×10^{15} $M_\odot$ (dashed).

factor connecting the smoothed linear overdensity with the primordial potential:

power-spectrum of a Gaussian gravitational potential

$$\mathcal{M}_R(k) = \frac{2}{3} \frac{T(k) k^2}{H_0^2 \Omega_{m,0}} W_R(k)$$

transfer function:

window function defining the radius R of a proto-halo of mass M(R):

Halo bias in NG models

- Extension to general (scale and configuration dependent) NG is straightforward

- In full generality write the ϕ bispectrum as $B_\phi(k_1,k_2,k_3)$. The relative NG correction to the halo bias is

$$\frac{\Delta b_h}{b_h} = \frac{\Delta_c(z)}{D(z)} \frac{1}{8\pi^2\sigma_R^2} \int dk_1 k_1^2 \mathcal{M}_R(k_1) \times$$
$$\int_{-1}^{1} d\mu \mathcal{M}_R\left(\sqrt{\alpha}\right) \frac{B_\phi(k_1,\sqrt{\alpha},k)}{P_\phi(k)} \times \frac{1}{M_R(k)}$$
$$\alpha = k_1^2 + k^2 + 2k_1 k\mu$$

- It also applies to non-local (e.g. “equilateral”) NG (DBI, ghost inflation, etc..) and universal NG term!!

Calibration on simulations

Grossi, Verde, Dolag, Branchini, Carbone, Iannuzzi, Matarrese & Moscardini 2009

Local non-Gaussianity

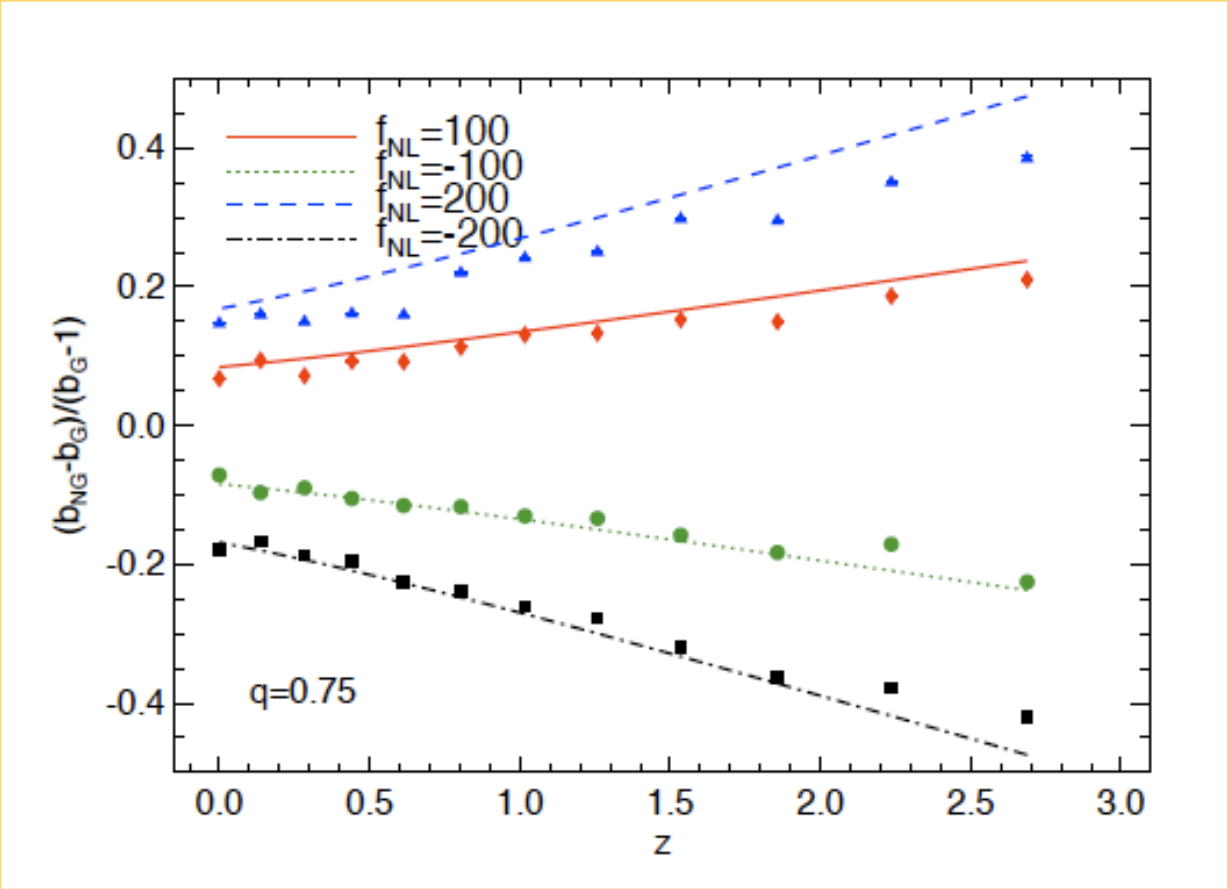

Observational prospects

On these large scales only the “two halo” term counts

Fisher matrix approach (Carbone, Verde & Matarrese 08):

From the P(k) shape

survey	z range	sq deg	mean galaxy density $(h/Mpc)^3$	$\Delta f_{\rm NL}/q'$ LSS
SDSS LRG's	$0.16 < z < 0.47$	7.6×10^3	1.36×10^{-4}	40
BOSS	$0 < z < 0.7$	10^4	2.66×10^{-4}	18
WFMOS low z	$0.5 < z < 1.3$	2×10^3	4.88×10^{-4}	15
WFMOS high z	$2.3 < z < 3.3$	3×10^2	4.55×10^{-4}	17
ADEPT	$1 < z < 2$	2.8×10^4	9.37×10^{-4}	→ 1.5
EUCLID	$0 < z < 2$	2×10^4	1.56×10^{-3}	→ 1.7
DES	$0.2 < z < 1.3$	5×10^3	1.85×10^{-3}	8
PanSTARRS	$0 < z < 1.2$	3×10^4	1.72×10^{-3}	3.5
LSST	$0.3 < z < 3.6$	3×10^4	2.77×10^{-3}	→ 0.7

ISW is found to be less powerful. See Afshordi & Tolley 08 for S/N

Observational status

Data/method	$f_{\rm NL}$	reference
Photometric LRG - bias	$63^{+54+101}_{-85-331}$	Slosar et al. 2008
Spectroscopic LRG- bias	$70^{+74+139}_{-83-191}$	Slosar et al. 2008
QSO - bias	8^{+26+47}_{-37-77}	Slosar et al. 2008
combined	28^{+23+42}_{-24-57}	Slosar et al. 2008
NVSS–ISW	$105^{+647+755}_{-337-1157}$	Slosar et al. 2008
NVSS–ISW	$236 \pm 127(2-\sigma)$	Afshordi&Tolley 2008
WMAP3-Bispectrum	30 ± 84	Spergel et al. (WAMP) 2007
WMAP3-Bispectrum	32 ± 68	Creminelli et al 2007
WMAP3-Bispectrum	87 ± 60	Yadav & Wandelt 2008
WMAP5-Bispectrum	51 ± 60	Komatsu et al. (WMAP) 2008
WMAP5-Minkowski	-57 ± 121	Komatsu et al. (WMAP) 2008

Local-type only, 2 σ errors

Observational prospects

Data/method	$\Delta f_{\rm NL}\ (1-\sigma)$	reference
BOSS–bias	18	Carbone et al 2008
ADEPT/Euclid–bias	1.5	Carbone et al 2008
PANNStarrs –bias	3.5	Carbone et al 2008
LSST–bias	0.7	Carbone et al 2008
LSST-ISW	7	Afshordi& Tolley 2008
BOSS–bispectrum	35	Sefusatti & Komatsu 2008
ADEPT/Euclid –bispectrum	3.6	Sefusatti & Komatsu 2008
Planck-Bispectrum	3	Yadav et al . 2007
BPOL-Bispectrum	2	Yadav et al . 2007

The bispectrum sees the “shape”, halo bias does not!

Non-Gaussianities in the IGM

Viel, Dolag, Branchini, Grossi, Matarrese & Moscardini 2008

Very first NG hydro simulations

NG initial conditions:

$$\Phi = \Phi_L + f_{NL}(\Phi_L^2 - \langle \Phi_L^2 \rangle)$$

$$\nabla^2(\Phi * T)g(z) = -4\pi G a^2 \delta\rho_{DM}$$

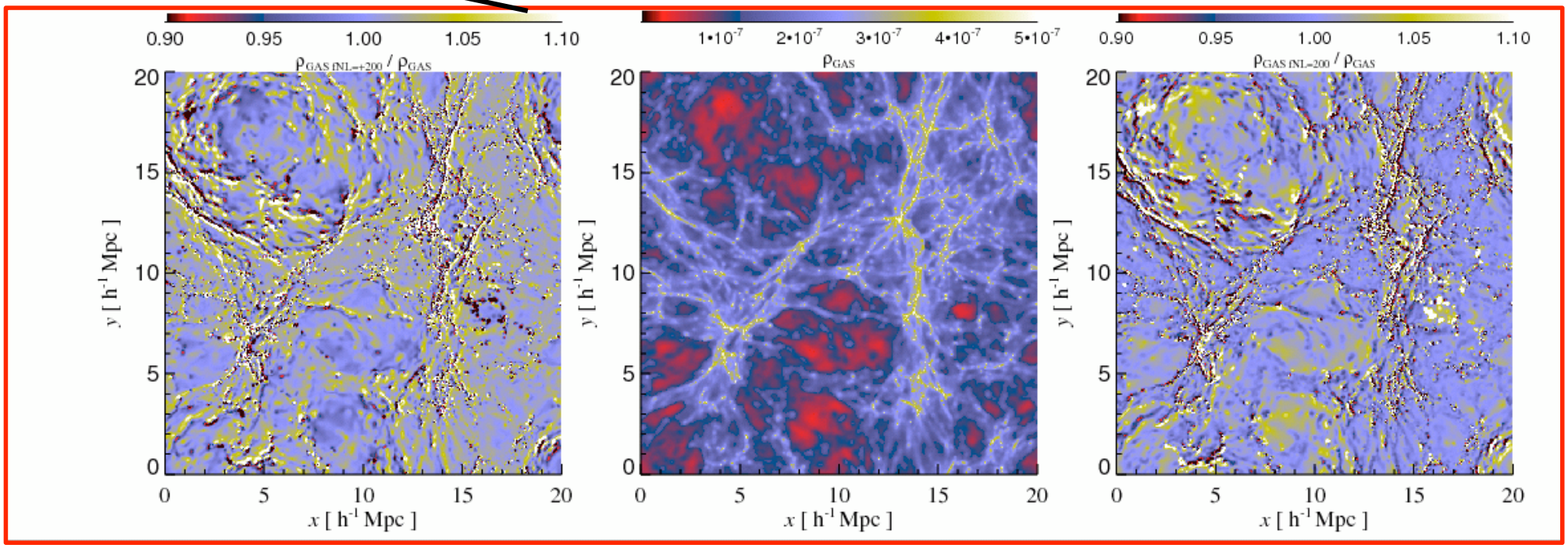

NG/G f_{NL} = 100 f_{NL} = 0 f_{NL} = - 100

GAS distribution in a slice of 3 Mpc/h (comoving) at z=3 (the voids have less and more matter compared to the standard case) – this in turn can be seen in the flux PDF

Conclusions

- Contrary to earlier naive expectations, some level of non-Gaussianity is generically present in *all inflation models*. The level of non-Gaussianity predicted in the simplest (single-field, slow-roll) inflation is slightly below the minimum value detectable by *Planck* and at reach of future galaxy surveys.

- Constraining/detecting non-Gaussianity is a powerful tool to discriminate among competing scenarios for perturbation generation (*standard slow-roll inflation, curvaton, modulated-reheating, DBI, ghost inflation, multi-field, etc. …*) some of which imply large non-Gaussianity. Non-Gaussianity will soon become the *smoking-gun* for non-standard inflation models.

- The *Planck* mission (*in combination with future galaxy surveys*) will open a new window to the physics of the early Universe.